A Channel-Estimate-Based Decision Feedback Equalizer Robust under Impulsive Noise

Konstantinos Pelekanakis and Mandar Chitre
Acoustic Research Laboratory, National University of Singapore, Singapore, 119223
E-mail: {costas, mandar}@arl.nus.edu.sg

***Abstract*—A channel-estimate-based decision feedback equalizer (CEB DFE) robust under impulsive noise is presented for single-input multiple-output (SIMO) underwater acoustic communications. Channel estimation is performed via the improved-proportionate M-estimate affine projection algorithm (IPMAPA), a linear complexity algorithm which is robust against impulsive interference and exploits channel sparseness. The superiority of IPMAPA to the normalized sign algorithm (NSA) and the normalized least-mean-square (NLMS) algorithm is demonstrated by processing data transmitted at 9 kbps over a $1.2\,\mathrm{km}$ shallow water environment contaminated by snapping shrimp noise.**

I. Introduction

There has been an increasing interest in using time-domain channel-estimate-based decision feedback equalizers (CEB-DFEs) for high-rate underwater acoustic communications [1-3]. This type of equalization allows explicit channel tracking rather than implicit, which is what the conventional DFE (direct adaptation based on the received signal) carries out. Thus, faster adaptation to channel variability is possible. Moreover, prior knowledge about the channel can be directly incorporated into the channel estimator for improved performance. For instance, exploiting channel sparseness can lead not only to better channel estimation accuracy but also to reduction of receiver complexity since only the significant channel taps can be retained in the equalization process.

Another reason for using a CEB DFE, which is often overlooked in underwater acoustic communications, is to gain robustness against impulsive noise. Most of the work, if not all, on channel estimation in underwater acoustic channels uses the L_2 norm of the channel prediction error (i.e., the difference between the observed signal and the adaptive filter output). However, a number of man-made and physical processes are impulsive. Examples are: ice cracking [4] and snapping shrimp noise [5]. Such environments require the use of robust adaptive filters since L_2 norm-based algorithms suffer severe performance degradation. Recently, the authors have introduced the improved-proportionate M-estimate affine projection algorithm (IPMAPA) [6], a linear complexity adaptive algorithm for channel estimation. This algorithm combines Hampel's three-part redescending M-estimate of the channel prediction error with natural gradient adaptation. This combination achieves robustness against impulsive noise while exploiting varying degrees of channel sparseness.

In this short communication, we incorporate the IPMAPA into a CEB DFE receiver, which jointly performs spatial diversity combining and adaptive Doppler compensation. Its effectiveness is confirmed by analyzing real data transmitted at 9 kbps over a $1.2\,\mathrm{km}$ shallow water channel contaminated by impulsive noise. In addition, we show that the IPMAPA outperforms the normalized sign algorithm (NSA) [7] and the normalized least-mean-square (NLMS) algorithm [8].

Notation: Superscripts $^\intercal$, †, and * stand for transpose, Hermitian transpose, and conjugate, respectively. Column vectors (matrices) are denoted by boldface lowercase (uppercase) letters.

II. System model and receiver architecture

The proposed communications system generates a 9 kbps baseband signal, expressed as

$$u(t) = \sum_{i=1}^{\infty} d(i) g(t - iT), \tag{1}$$

where $\{d(i)\}$ denotes the 8-PSK symbol sequence and $g(t)$ represents the response of the (pulse-shaping) raised cosine filter with signaling interval T=1/3,000 s and roll-off factor α=0.7. Before transmission, the baseband signal is modulated onto a carrier f_c=17,000 Hz and the resulting passband signal occupies the frequency range 14.4-19.5 kHz. The passband signal travels through the underwater channel and undergoes delay spread due to multipath propagation and Doppler spread due to the relative motion between the transmitter and the receiver.

The received signal is shifted to baseband, low-pass filtered and coarsely synchronized with a known chirp signal. Assuming that all acoustic paths arriving at sensor m experience the same time scale effect, the received baseband signal can be written as

$$r^m(t) = \sum_{\ell} s_\ell^m(t) u(t + \Delta^m t - \tau_\ell^m) e^{j2\pi f_c(\Delta^m t - \tau_\ell^m)} + z^m(t) \tag{2}$$

where $s_\ell^m(t)$ denotes the attenuation (along path ℓ), Δ^m stands for the time scale difference between the transmitter and the receiver, τ_ℓ^m represents the ℓ-th path delay within a symbol interval, and $z^m(t)$ denotes the additive noise process.

The proposed receiver architecture can be seen in Figure 1. There are three processing stages: adaptive resampling based on mean Doppler shift estimation, post-cursor inter-symbol interference (ISI) mitigation based on robust channel estimation and adaptive linear equalization.

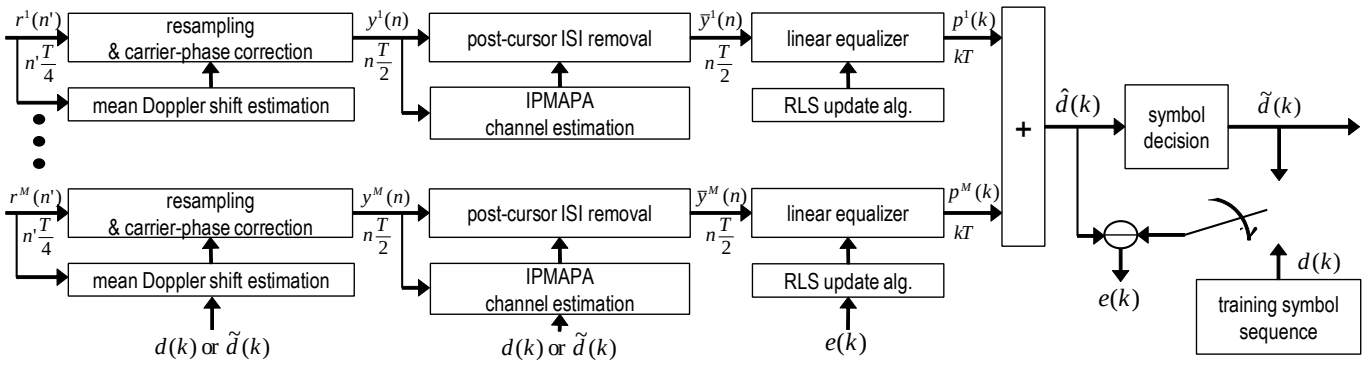

Fig. 1. Block diagram of receiver.

A. Adaptive resampling

Assuming that the relative motion between the transmitter and receiver is significant, then the received signal is time-scaled (compressed or dilated) with respect to the transmitted signal [9]. To compensate for the mean Doppler shift, we change the sampling rate of the baseband signal by using linear interpolation [10]. Let us denote $r^m(n')$ the discrete sampled baseband signal sampled at four samples/symbol. The output of the linear interpolator is downsampled to two samples/symbol, denoted as $y^m(n)$ and is given by

$$y^m(n) = I^m(k)r^m(n')+(I^m(k)-1)r^m(n'+1) \quad (3)$$
$$I^m(k) = I^m(k-1) + K_1\theta^m(k) \quad (4)$$
$$\theta^m(k) = \mathrm{Im}\left\{p^m(k)\tilde{d}(k)^*\right\} \quad (5)$$

where n'={1,3,...}, n={1,2,...}, $I^m(k)$ is the one-tap linear interpolator updated at the symbol rate ($I^m(0)$=1), $\tilde{d}(k)$ denotes the decided symbol when the DFE operates in decision-directed mode, $p^m(k)$ is the output of the feedforward filter and K_1 is a phase tracking parameter.

B. Robust channel estimation

After mitigating for the mean Doppler shift, the received signal sampled at time n can be written in vector form as

$$y^m(n) = \mathbf{h}^m(n)^\dagger \mathbf{u}(n) + z^m(n), \quad (6)$$

with $\mathbf{u}(n)$=$[u(n-N_c+1)\dots u(n)...u(n+N_a)]^\intercal$ and $\mathbf{h}^m(n)$=$[h^m(n,N_c-1)...h^m(n,0)...h^m(n,-N_a)]^\intercal$ are the samples of the input signal in (1) and the m-th channel impulse response, respectively. The parameters N_c, N_a denote, respectively, the causal and acausal taps of the channel impulse response. The element $h^m(n,0)$ denotes the channel tap with maximal amplitude.

Let us assume that $z^m(n)$ is Gaussian noise plus impulsive interference. If an impulse corrupts the receiver, it can be detected with high probability in the prior error signal $e^m(n)$=$y^m(n)-\hat{\mathbf{h}}^m(n-1)^\dagger\mathbf{u}(n)$, where $\hat{\mathbf{h}}^m(n)$ is the estimate of $\mathbf{h}^m(n)$. The IPMAPA is a sparse adaptive algorithm with the ability to detect and downweight noise impulses via the function [6]

$$q(e) = \begin{cases} 1 & ,0 \le |e|_2 < \xi \\ \dfrac{\xi}{|e|_2} & ,\xi \le |e|_2 < \Delta \\ \xi\dfrac{|e|_2 - T}{\Delta - T}\dfrac{1}{|e|_2} & ,\Delta < |e|_2 < T \\ 0 & ,T < |e|_2 \end{cases}.$$

The threshold parameters ξ, Δ,and T are continuously estimated under the assumption of contaminated Gaussian noise. The channel update equations are summarized below (superscript m is omitted for brevity):

$$\mathbf{e}(n)^* = \mathbf{y}(n)^* - \mathbf{U}(n)^\dagger\hat{\mathbf{h}}(n-1), \quad (7)$$
$$\mathbf{A}(n) = \mathbf{G}(n-1)\mathbf{U}(n), \quad (8)$$
$$\mathbf{B}(n) = \left(\mathbf{U}(n)^\dagger\mathbf{A}(n) + \delta\,\mathbf{Q}(n)^{-1}\right)^{-1}, \quad (9)$$
$$\hat{\mathbf{h}}(n) = \hat{\mathbf{h}}(n-1) + \mu\mathbf{A}(n)\mathbf{B}(n)\mathbf{e}(n)^*, \quad (10)$$

where $\mathbf{y}(n)$=$[y(n)\,y(n-1)\dots y(n-L+1)]^\intercal$ contains the L most recent output samples (usually $L \le$10), $\mathbf{U}(n)$=$[\mathbf{u}(n)\,\mathbf{u}(n-1)\dots\mathbf{u}(n-L+1)]$ is the $(N_c+N_a)\times L$ matrix of input samples, $\mathbf{G}(n)$ is diagonal matrix that exploits sparseness[1], $\mathbf{Q}(n)$ is an $L\times L$ diagonal matrix with elements $q(e(n)),...,q(e(n-L+1))$ and $\mu \in (0,1]$ is the step-size parameter. Initialization of the algorithm starts with $\hat{\mathbf{h}}(0)$=$\mathbf{0}$. Note that the IPMAPA exhibits $O(N_c+N_a)$ computational complexity since $\mathbf{G}(n)$ is diagonal and $N_c+N_a \gg L$.

C. Equalization

Let L_c, L_a denote, respectively, the causal and acausal taps of the feedforward section of the equalizer and let $\mathbf{y}^m(n) = [y^m(n-L_c+1)\dots y^m(n)...y^m(n+L_a)]^\intercal$ be the vector of received samples. Here, we follow the idea of post-cursor ISI cancellation by combining previous channel

[1]The purpose of $\mathbf{G}(n)$ is to assign a variable step size parameter to each filter tap [6]. This parameter is a function of the tap's previously estimated magnitude. As a result, active filter taps (i.e., taps with significant values) converge fast, which makes the overall algorithm to have fast convergence.

estimates and symbol decisions before adaptive feedforward equalization [2]. The received signal can be written as

$$\mathbf{y}^m(n) = \mathbf{H}^m(n)\mathbf{x}(n) + \mathbf{z}^m(n), \tag{11}$$

where $\mathbf{x}(n)$=$[u(n - N_c - L_c + 2) \dots u(n)...u(n + N_a + L_a)]^\intercal$, $\mathbf{z}^m(n)$=$[z^m(n-L_c+1) \dots z^m(n)...z^m(n+L_a)]^\intercal$ and $\mathbf{H}^m(n)$ is the channel matrix with the j-th row composed of $\mathbf{h}^m(n-L_c+j)^\dagger$. Let us now partition the channel matrix into causal and acausal parts as follows: $\mathbf{H}^m(n)$=$[\mathbf{H}_c^m(n)|\mathbf{H}_{ac}^m(n)]$. The ISI-free signal at the input of the feedforward filter can be constructed by subtracting previous channel estimates and symbol decisions as follows:

$$\bar{\mathbf{y}}^m(n) = \mathbf{y}^m(n) - \hat{\mathbf{H}}_c^m(n)\mathbf{x}_c(n), \tag{12}$$

where $\mathbf{x}_c(n)$ is the causal part of the input signal. The soft estimate, $\hat{d}(k)$, of the transmitted symbol is obtained by summing the outputs of all feedforward filters, i.e., $\hat{d}(k)$=$\sum_{m=1}^{M} p^m(k)$. The exponentially-weighted RLS algorithm [8] is used to jointly adapt the feedforward filters based on the error $\hat{d}(k)$-$\tilde{d}(k)$.

III. Experimental results and discussion

We now report on the performance of the receiver, which jointly performs multi-sensor combining, Doppler compensation and CEB DFE. To evaluate the effectiveness of IPMAPA, we compare it with two standard linear complexity channel estimation algorithms: the NLMS and the NSA. The NLMS algorithm is not robust under impulsive noise and does not exploit channel sparseness. The NSA is based on the L_1 norm of the error signal and thus, it is robust under impulsive noise.

The dataset analyzed here was recorded during a sea trial in the area of Selat Pauh in Singapore waters. Figure 2(a) shows the transmit/receive locations. The distance of the link was $1.2\,\mathrm{km}$. The receiver used a horizontal uniformly-spaced linear array of 19 hydrophones ($4.57\,\mathrm{cm}$ inter-element spacing). Both the array and the transmitter were mounted on two vessels and submerged about $3\,\mathrm{m}$ below the sea surface. The sea depth at the receiver location was about $20\,\mathrm{m}$ and the sound speed profile was isovelocity ($1540\,\mathrm{m/s}$). We stress three notable characteristics of this link: (a) impulsive ambient noise due to snapping shrimp, (b) strong tidal currents and (c) frequent ship wakes as this area was exposed to heavy shipping traffic.

Figure 2(b) validates the impulsiveness of the passband ambient noise in the frequency range 14.4-19.5 kHz. It can be clearly seen that the Symmetric alpha-Stable (SαS) distribution (with characteristic function $\varphi(\omega)$=$e^{-\gamma^\alpha|\omega|^\alpha}$, α=1.65 and γ=0.2) is a better fit than the Gaussian distribution. Figure 2(c) shows the amplitudes of the received baseband signals at sensors 2 and 19. The impulsiveness of the noise can be clearly seen. The SNR at each sensor is about 19 dB.

Figure 2(d) shows the mean Doppler shifts experienced by sensors 2 and 19. Clearly, the Doppler shifts are highly correlated since the sensors are only $78\,\mathrm{cm}$ apart. This oscillatory fluctuation of the Doppler frequency is due to the wave-induced motion of the receive and transmit vessels.

The time evolution of the channel impulse response as seen by sensor 2 of the array is illustrated in Figure 2(e). The $0\,\mathrm{ms}$ delay corresponds to the strongest arrival. As can be observed, the multipath arrivals are very sparse and the total multipath spread the transmitting signal experiences is about $85\,\mathrm{ms}$. The sound rays arriving at $85\,\mathrm{ms}$ after the direct arrival are generated due to reflections off a reef behind the transmit vessel as seen from Figure 2(a). For a sampling rate of 2 samples/symbol, the required length of an adaptive filter to capture the entire multipath is 607 taps.

The impact of the aforementioned channel estimation algorithms on the performance of the CEB DFE is illustrated in Figure 2(f). Specifically, we compute the SER (symbol error rate) and the output SNR of the CEB DFE, defined as

$$SNR_{out} = 10\log\frac{E[|d(k)|^2]}{\frac{1}{N}\sum_{k=1}^{N}\left|d(k)-\hat{d}(k)\right|^2}, \tag{13}$$

for an increasing number of sensors. For these results, the feedforward filter associated with each sensor has 13 taps and all feedforward filters are jointly adapted via the RLS algorithm. In addition, 1000 symbols are used for training. Note that both NLMS and NSA fail regardless the number of sensors. In contrast, IPMAPA gives good SER/SNR_{out} performance when one sensor is employed but its performance drastically improves when two sensors are used. As more sensors are employed, the IPMAPA receiver demonstrates slightly better SNR_{out} performance due to the limited spatial diversity (signals are highly coherent among the sensors). In addition, note that the SER slightly reduces when sensors 2, 12,19 are used as compared to senors 2,19. This is attributed to the fact that strong impulses affect different sensors at different times. Finally, Figure 2(f) shows the scatter plot at the output of the CEB DFE when IPMAPA and four sensors (2,7,12,19) are used.

IV. Conclusion

An improved CEB DFE receiver robust in impulsive noise was proposed. The receiver was based on IPMAPA, a linear complexity channel estimation algorithm which is robust under impulsive noise and manages to exploit varying degrees of channel sparseness. Three CEB DFE structures based on IPMAPA, NLMS and NSA were compared. The superiority of the IPMAPA was demonstrated in real data transmitted at 9 kbps over a $1.2\,\mathrm{km}$ shallow water link contaminated by snapping shrimp noise.

Acknowledgment

This research was supported by the MINDEF/NUS/JPP/13/01/04 grant. The authors are indebted to Mr. Zou Nan and Mr. Gimhwa Chua of DSO National Laboratories for their leadership during the sea trials in Singapore.

(a)

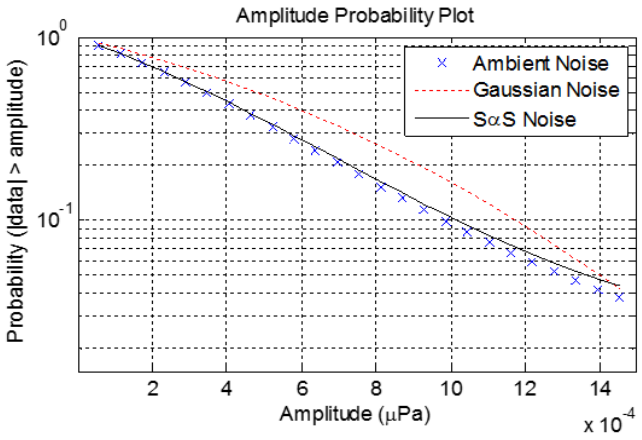

(b)

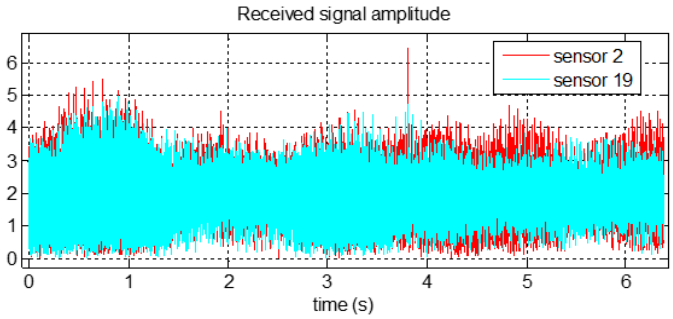

(c)

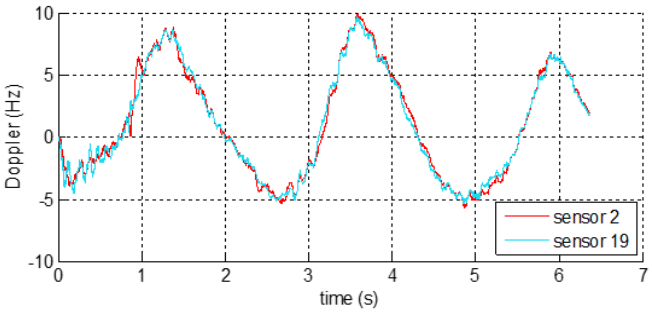

(d)

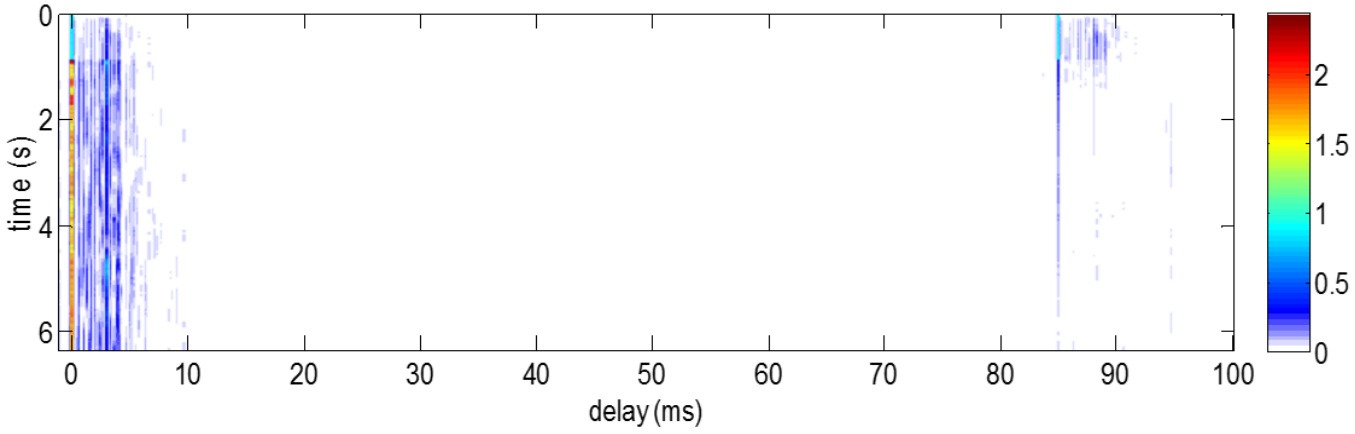

(e)

	sensor # = 2 SNR_{out} (dB) SER	sensor # = 2,19 SNR_{out} (dB) SER	sensor # = 2,12,19 SNR_{out} (dB) SER	sensor # = 2,7,12,19 SNR_{out} (dB) SER
NLMS	-0.8 dB 10446/18097	-1.6 dB 10681/18097	-0.1 dB 10127/18097	-1.3 dB 10606/18097
NSA	-1.7 dB 12307/18097	-0.8 dB 8639/18097	-0.5 dB 11157/18097	-1.4 dB 10810/18097
IPMAPA	12.2 dB 448/18097	15.6 dB 23/18097	15.8 dB 30/18097	16.0 dB 26/18097

(f)

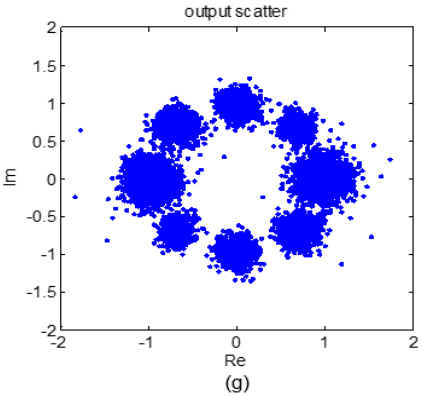

(g)

Fig. 2. (a) Map of experimental link. (b) Goodness of fit of passband ambient noise series to SαS and Gaussian distribution. (c) Time series of received baseband signal as seen by sensors 2 and 19. (d) Doppler vs. time for sensors 2 and 19. (e) Snapshots of the channel response. The x-axis shows multipath delay, the y-axis shows absolute time and the z-axis shows the channel amplitude in linear scale. The snapshots are generated at the symbol rate. (f) SNRout / SER vs. number of sensors. (g) Scatter plot at the output of the equalizer.

REFERENCES

[1] J. C. Preisig, "Performance analysis of adaptive equalization for coherent acoustic communications in the time-varying ocean environment," *J. Acoust. Soc. Amer.*, vol. 118, pp., 263-278, 2005.

[2] M. Stojanovic, “Efficient processing of acoustic signals for high rate information transmission over sparse underwater channels,” *J. Phys. Commun.*, pp. 146-161, 2008.

[3] J. Tao et al, "Channel estimation, equalization and phase correction for single carrier underwater acoustic communications," *in Proc. MTS/IEEE OCEANS Conf.*, Japan, 2008.

[4] M. Bouvet and S. C. Schwartz, "Comparison of adaptive and robust receivers for signal detection in ambient underwater noise," *IEEE Trans. Acoust., Speech, Signal Processing*, vol. ASSP-37, pp. 621-626, 1989.

[5] K. Pelekanakis and M. Chitre, “A Class of Affine Projection Filters that Exploit Sparseness under Symmetric alpha-Stable noise”, *in Proc. MTS/IEEE Conf.*, Norway, 2013.

[6] K. Pelekanakis, M. Chitre, "Adaptive Sparse Channel Estimation under Symmetric alpha-Stable Noise," *Wireless Communications, IEEE Transactions on*, vol.13, no.6, pp. 3183-3195, 2014.

[7] O. Arikan, A. E. Cetin, and E. Erzin, “Adaptive filtering for non-Gaussian stable processes,” IEEE Signal Process. Lett., vol. 1, no. 11, pp. 163–165, Nov. 1994.

[8] S. Haykin, Adaptive Filter Theory, 4th ed. Upper Saddle River, NJ: Prentice-Hall, 2002.

[9] T. Riedl and A. Singer, "MUST-READ: Multichannel sample-by-sample turbo resampling equalization and decoding," *in Proc. MTS/IEEE Conf.*, Norway, pp. 1-5, 2013.

[10] C. P. Shah, C. C. Tsimenidis, B. S. Sharif, J. A. Neasham, "Low-Complexity Iterative Receiver Structure for Time-Varying Frequency-Selective Shallow Underwater Acoustic Channels Using BICM-ID: Design and Experimental Results," *Oceanic Engineering, IEEE Journal of*, vol.36, no.3, pp. 406-421, 2011.